STEM CELLS TRANSLATIONAL MEDICINE®

TISSUE-SPECIFIC PROGENITOR AND STEM CELLS

# Propranolol Targets Hemangioma Stem Cells via cAMP and Mitogen-Activated Protein Kinase Regulation

NAIKHOBA C.O. MUNABI,[a,*] RYAN W. ENGLAND,[a,*] ANDREW K. EDWARDS,[a] ALISON A. KITAJEWSKI,[a] QIAN KUN TAN,[a] ANDREW WEINSTEIN,[a] JUSTIN E. KUNG,[a] MAYA WILCOX,[a] JAN K. KITAJEWSKI,[b,c,d] CARRIE J. SHAWBER,[a,b,d] JUNE K. WU[a]

**Key Words.** Hemangioma • Propranolol • β-Adrenergic receptor • Cell proliferation • Cell death • Mitogen-activated protein kinase • cAMP • Stem cell

[a]Department of Surgery, [b]Department of Obstetrics and Gynecology, [c]Department of Pathology and Cell Biology, and [d]Herbert Irving Comprehensive Cancer Center, Columbia University College of Physicians and Surgeons, New York, New York, USA

[*]Contributed equally.

Correspondence: June K. Wu, M.D., F.A.C.S., Department of Surgery, Columbia University College of Physicians and Surgeons, 161 Fort Washington Avenue, Suite 511, New York, New York 10032, USA. Telephone: 212-342-3704; E-Mail: jw92@cumc.columbia.edu

Received April 16, 2015; accepted for publication September 18, 2015; published Online First on November 16, 2015.


1066-5099/2015/$20.00/0

http://dx.doi.org/10.5966/sctm.2015-0076

## ABSTRACT

**Infantile hemangiomas (IHs) are the most common vascular tumor and arise from a hemangioma stem cell (HemSC). Propranolol has proved efficacious for problematic IHs. Propranolol is a nonselective β-adrenergic receptor (βAR) antagonist that can lower cAMP levels and activate the mitogen-activated protein kinase (MAPK) pathway downstream of βARs. We found that HemSCs express β1AR and β2AR in proliferating IHs and determined the role of these βARs and the downstream pathways in mediating propranolol's effects. In isolated HemSCs, propranolol suppressed cAMP levels and activated extracellular signal-regulated kinase (ERK)1/2 in a dose-dependent fashion. Propranolol, used at doses of $<10^{-4}$ M, reduced cAMP levels and decreased HemSC proliferation and viability. Propranolol at $\geq 10^{-5}$ M reduced cAMP levels and activated ERK1/2, and this correlated with HemSC apoptosis and cytotoxicity at $\geq 10^{-4}$ M. Stimulation with a βAR agonist, isoprenaline, promoted HemSC proliferation and rescued the antiproliferative effects of propranolol, suggesting that propranolol inhibits βAR signaling in HemSCs. Treatment with a cAMP analog or a MAPK inhibitor partially rescued the HemSC cell viability suppressed by propranolol. A selective β2AR antagonist mirrored propranolol's effects on HemSCs in a dose-dependent fashion, and a selective β1AR antagonist had no effect, supporting a role for β2AR signaling in IH pathobiology. In a mouse model of IH, propranolol reduced the vessel caliber and blood flow assessed by ultrasound Doppler and increased activation of ERK1/2 in IH cells. We have thus demonstrated that propranolol acts on HemSCs in IH to suppress proliferation and promote apoptosis in a dose-dependent fashion via β2AR perturbation, resulting in reduced cAMP and MAPK activation.** STEM CELLS TRANSLATIONAL MEDICINE *2016;5:45–55*

## SIGNIFICANCE

The present study investigated the action of propranolol in infantile hemangiomas (IHs). IHs are the most common vascular tumor in children and have been proposed to arise from a hemangioma stem cell (HemSC). Propranolol, a nonselective β-adrenergic receptor (βAR) antagonist, has proven efficacy; however, understanding of its mechanism of action on HemSCs is limited. The presented data demonstrate that propranolol, via βAR perturbation, dose dependently suppresses cAMP levels and activated extracellular signal-regulated kinase 1/2. Furthermore, propranolol acts via perturbation of β2AR, and not β1AR, although both receptors are expressed in HemSCs. These results provide important insight into propranolol's action in IHs and can be used to guide the development of more targeted therapy.

## INTRODUCTION

Infantile hemangiomas (IHs) are benign vascular tumors affecting approximately 4%–10% of infants [1, 2]. The natural history of IHs is well documented and includes rapid proliferation in the first months of life, a plateau phase up to approximately 1 year, followed by involution into a fibrofatty residuum by early childhood [3]. Although IHs are benign and eventually undergo spontaneous regression, rapid growth of the tumor during the proliferative phase can result in serious morbidity and even mortality. Complications can include bleeding and congestive heart failure, permanent visual impairment, and unstable airway obstruction, leading to respiratory distress [4–8].

Propranolol, a nonselective β-adrenergic receptor (βAR) antagonist, has been found to be

an effective drug for treating IH [9–13]. Despite its efficacy in treating the morbidities of IH, adverse effects have been described, including symptomatic bradycardia, hypotension, hypoglycemia, and hypoglycemia-induced seizures [14, 15]. The mechanisms of action of propranolol in IHs have yet to be fully elucidated. It has been proposed that its effects are mediated via $\beta$AR inhibition on two cell types in IHs, hemangioma stem cells (HemSCs) and hemangioma endothelial cells (HemECs). Greater knowledge of the mechanism by which propranolol affects IHs could guide the development of therapies that minimize the potential adverse effects and maximize efficacy.

Studies of propranolol using IH-derived cells have suggested that it targets multiple cell types in IHs. Propranolol has antiproliferative and antiangiogenic effects on HemECs [16–18] and antiproliferative and increased contractility on IH-derived $\alpha$-smooth muscle actin-positive mural cells [19]. Propranolol has been shown to induce the death of HemSCs, the cell type proposed to be the origin of IHs [20–23].

$\beta$ARs are G-protein-coupled receptors that promote cellular proliferation and survival [17, 18, 24–27]. In cultured endothelial or tumor cells, propranolol has been shown to both reduce cAMP levels and simultaneously activate the mitogen-activated protein kinase (MAPK) pathway downstream of $\beta$AR inhibition [24–28]. Propranolol lowers cAMP levels by inhibiting the G$\alpha$s/adenylyl cyclase downstream pathway [28]. Propranolol activation of extracellular signal-regulated kinase (ERK)1/2 is thought to be independent of a G-protein pathway, possibly involving $\beta$-arrestins [29–33]. The roles of cAMP and ERK1/2 regulation subsequent to propranolol treatment in HemSCs have yet to be fully elucidated.

In the present study, we examined the mechanisms by which propranolol affects HemSC cellular behavior, with a focus on the downstream $\beta$AR signaling pathways involving cAMP and MAPK. We demonstrate that propranolol reduces cAMP levels and activates ERK1/2 in HemSCs in a dose-dependent manner. At lower concentrations ($<10^{-4}$ M), propranolol suppression of cAMP levels correlated with reduced HemSC proliferation. At higher concentrations ($\geq 10^{-5}$ M), propranolol reduced cAMP levels and increased ERK1/2 activity, which correlated with HemSC apoptosis and cytotoxicity at the $>10^{-4}$ M concentration. Experiments using isoprenaline ($\beta$AR agonist), bucladesine (cAMP analog), and U0126 (MAPK inhibitor) partially rescued the HemSC viability suppressed by propranolol. Propranolol's effects on HemSCs were primarily mediated through $\beta$2ARs, because ICI-118,551 (ICI), a $\beta$2-specific adrenergic receptor antagonist, mirrored that of propranolol. Finally, using an IH mouse model, we have demonstrated that propranolol rescues abnormal blood vessel development and activates ERK1/2 in vivo. Taken together, our results suggest that propranolol mediates its effects on HemSCs by inhibiting $\beta$AR signaling to suppress cAMP levels and induce MAPK signaling.

## Materials and Methods

### Tissue Collection and Cell Culture

The Columbia University institutional review board approved the collection and use of tissues (protocol no. IRB-AAA9976). Preparation of hemangioma specimens for immunohistochemistry consisted of overnight fixation in 4% paraformaldehyde, sucrose soaking, and freezing in Tissue-Tek O.C.T. compound (Sakura Finetek, Tokyo, Japan, http://www.sakura-finetek.com) 7-$\mu$M frozen sections were made. HemSC isolation was performed, and HemSCs were characterized as described previously [21]. In brief, tissues with regions of proliferating IH (supplemental online Table 1) were disassociated with collagenase, and HemSCs were selected by CD133+ magnetic bead isolation (Miltenyi Biotec, Bergisch Gladbach, Germany, http://www.miltenyibiotec.com). HemSCs were cultured in Endothelial Cell Growth Medium-2 (EGM-2; Lonza, Walkersville, MD, http://www.lonza.com) with 20% fetal bovine serum (FBS; Life Technologies, Carlsbad, CA, http://www.lifetechnologies.com). Bone marrow-derived mesenchymal stem cells (MSCs) were purchased (Lonza) and grown in EGM-2 with 20% FBS. Three cell lines were tested for each assay (supplemental online Table 1).

### Immunohistochemistry

Fixed frozen IH tissue sections and IH xenograft tissues were stained as previously described [34]. The antibodies included $\beta$1AR (1:400; Abcam, Cambridge, U.K., http://www.abcam.com) and $\beta$2AR (1:500; Abcam), CD133 (1:50; EMD Millipore, Billerica, MA, http://www.emdmillipore.com), CD31 (1:50; Dako, Glostrup, Denmark, http://www.dako.com), and phosphorylated ERK1/2 (pERK1/2) (P-p44/42; 1:100; Cell Signaling Technology, Beverly, MA, http://www.cellsignal.com) and were detected with either Alexa Fluor 488 or 594 secondary antibodies (Invitrogen, Carlsbad, CA, http://www.invitrogen.com). From each IH xenograft, the number of activated ERK1/2-positive cells was determined and divided by the total number of cells from three representative high-power fields (HPFs).

### Reagents

Propranolol hydrochloride (Sigma-Aldrich, St. Louis, MO, http://www.sigmaaldrich.com) was reconstituted at 100 mM in pH 3.0 water. Atenolol (Sigma-Aldrich) was reconstituted at 50 mM in dimethyl sulfoxide (DMSO). ICI-118,551 hydrochloride (Sigma-Aldrich) was reconstituted at 25 mM in sterile pH 7.0 water. Isoprenaline hydrochloride (Sigma-Aldrich) and dibutyryl cyclic adenosine monophosphate (bucladesine; R&D Systems, Minneapolis, MN, http://www.rndsystems.com), a cAMP analog, were both reconstituted in water to a concentration of 100 mM. U0126, a MEK1/MEK2 inhibitor, was reconstituted in DMSO to a concentration of 25 mM.

### cAMP Assay

The cAMP levels in HemSCs were determined using the LANCE *Ultra* cAMP kit (PerkinElmer Life and Analytical Sciences, Waltham, MA, http://www.perkinelmer.com). The HemSCs were washed and resuspended in the provided stimulation buffer (Hanks' balanced saline solution, bovine serum albumin, isobutylmethylxanthine, HEPES buffered saline solution) and seeded (1,000 per well) on a 96-well plate. The cells were then treated with drugs for 30 minutes. Tracer and U*Light*-anti-cAMP working solutions were added and incubated at room temperature for 1 hour. The time-resolved fluorescence resonance energy transfer signal was determined using the EnVision Multilabel Plate Reader (PerkinElmer Life and Analytical Sciences). cAMP levels were determined using a standard curve, and data were interpolated using a comprehensive curve fitting (nonlinear regression) and Prism (GraphPad Software, Inc., San Diego, CA, http://www.graphpad.com). Each condition was used in triplicate, and the experiments were

 

performed at least two times. A representative experiment is presented in the figures.

To determine whether βARs are coupled to Gαs or Gαi in HemSCs, the cells were treated with isoprenaline, with or without 10 μM forskolin, over a 6-log dose range by serial dilutions with water for 30 minutes. Next, the cAMP levels were measured as described to determine whether βARs were coupled to Gαs or Gαi in HemSCs.

### ERK1/2 Western Blotting

Cells were cultured on fibronectin-coated plates and treated with various concentrations of βAR antagonists and incubated for 30 minutes. The cells were lysed in TENT buffer (50 mM Tris [pH 8.0], 2 mM EDTA, 150 mM NaCl, 1% Triton-X-100) with 1% Halt Protease Inhibitor (Thermo Scientific, Wilmington, DE, http://www.thermoscientific.com), 1% phosphatase inhibitor (Thermo Scientific), and 0.5% sodium orthovanadate (FIVEphoton Biochemicals, San Diego, CA, http://www.fivephoton.com). Western blotting was performed for ERK1/2 (p44/42, 1:1,000; Cell Signaling Technology) and pERK1/2 (P-p44/42, 1:500; Cell Signaling Technology). The blots were stripped and then probed for α-tubulin (1:10,000; Sigma-Aldrich) to normalize protein loading. Experiments were performed at least three times, and a representative experiment is presented in the figures.

### Proliferation Assay

HemSCs (5,000–10,000 per well) were seeded at subconfluency on a fibronectin-coated 24-well plate in EGM-2 with 20% FBS. Four hours later, the media were removed and the cells treated with various concentration of drug in serum-free media (SFM; Life Technologies) supplemented with 1% FBS. After 24–72 hours, the cell number was determined using the Cell Counting Kit-8 (Dojindo Molecular Technologies Inc., Gaithersburg, MD, http://www.dojindo.com) and using a standard curve. Each condition was used in triplicate, and the experiments performed at least three times. A representative experiment is presented in the figures.

### Cytotoxicity/Digital Imaging Microscopy System Assay

HemSCs (4,000 cells per well) were seeded on a fibronectin-coated 96-well plate in EGM-2 with 20% FBS. The next day, when the HemSCs had reached confluence, the media were removed, and cells were treated with various concentrations of drug in SFM with 0.1% FBS. After 24 hours, the cells were incubated in 10 μg/ml fluorescein diacetate and 0.5% Eosin-Y for 20 minutes. Cell viability was determined by fluorescence using the Digital Imaging Microscopy System (DIMSCAN; BioImaging Solutions, Inc., San Diego, CA, http://www.bioimagimgsolutions.com) [35]. Each condition was used in triplicate or sextuplet, and experiments were performed at least three times. A representative experiment is presented in the figures.

### Apoptosis Assays

#### Annexin V Assay

HemSCs were seeded in EGM-2 with 20% FBS media on 6-$cm^2$ plates. After 4 hours, increasing concentrations of propranolol in SFM with 0.1% FBS were added to HemSCs. After 6 hours, Annexin V expression levels were measured using the Annexin V-FITC Apoptosis Kit (BioVision, Inc., Milpitas, CA, http://www.biovision.com). Antibody detection was performed using the FACSCalibur flow cytometer (BD Biosciences).

#### Caspase-3 Assay

HemSCs were seeded in EGM-2 with 20% FBS media and allowed to settle for 4 hours. HemSCs were treated at increasing concentrations of propranolol in SFM with 0.1% FBS for 24 hours. The protein lysates were collected, and caspase-3 activation was quantified using the Caspase-3 Human ELISA Kit (Life Technologies).

### IH Mouse Model

All animal studies were performed with approval from Columbia University's institutional animal care and use committee (approval no. AAAG5852). To study the effects of propranolol on HemSCs in vivo, a xenograft mouse model of IH was used as previously described [20]. In brief, $1.5 \times 10^6$ HemSCs ($n$ = 2) suspended in 200 μL of Corning Matrigel Matrix (Corning, Corning, NY, http://www.corning.com) was implanted subcutaneously into the flanks of female 6–8-week-old NCrNude immunodeficient mice ($n$ = 4; Taconic Biosciences, Hudson, NY, http://www.taconic.com). Propranolol, which was provided in drinking solution, was initiated the day of IH xenografting. Propranolol was diluted to 270 μM in 5% dextrose water (vehicle), and daily consumption was measured to calculate the treatment dosage, which averaged 40 mg/kg daily.

Blood flow within the IH Matrigel implant was analyzed using a VEVO 2100 Ultrasound Imaging System (VisualSonics, Toronto, ON, Canada, http://www.visualsonics.com) on a Doppler setting on days 14 and 21 of IH development. The mice were anesthetized with isoflurane and restrained in a supine position. The region of interest was fully scanned, with the transducer positioned at its largest longitudinal section over the implant to optimize the spatial resolution of the image, maximizing the detail. Next, two-dimensional images were captured in uniform steps of 0.05 mm. The images of blood flow were analyzed using software provided by VisualSonics.

The mice were sacrificed after 21 days. The Matrigel implants were collected and fixed overnight at 4°C in 10% formalin. The implants were dehydrated and embedded in paraffin for histological analysis. Vessel density and caliber were counted in 3–4 HPFs per implant ($n$ = 4 for each group). Vessel density was determined as the number of vessels (whether longitudinally or axially oriented) per HPF. The vessel diameter was measured according to the orientation. For longitudinally oriented vessels, the width was measured at three points and averaged, and the cross-section (axial) vessels were measured once. Vessels were identified as tubular structures with erythrocytes within.

### Statistical Analysis

To determine the significance between the control and experimental groups in the in vitro studies, a two-sample independent measures $t$ test was used. For analyses of more than two groups, analysis of variance (ANOVA) with the Tukey-Kramer post hoc test (family error rate, $\alpha$ = 0.05) was performed. The caspase-3 assay significance was determined for a series of four two-sample independent measures $t$ tests with Bonferroni's correction (family error rate, $\alpha$ = 0.05, corresponding to an individual hypothesis test error rate of $\alpha$ = 0.0127). Cohen's $d$, which reflects the magnitude of the treatment effect, was calculated and reported; by convention, $d > 0.8$ corresponds to a large effect size. For in vivo studies, the nonparametric Mann-Whitney $U$ test was used to compare

 

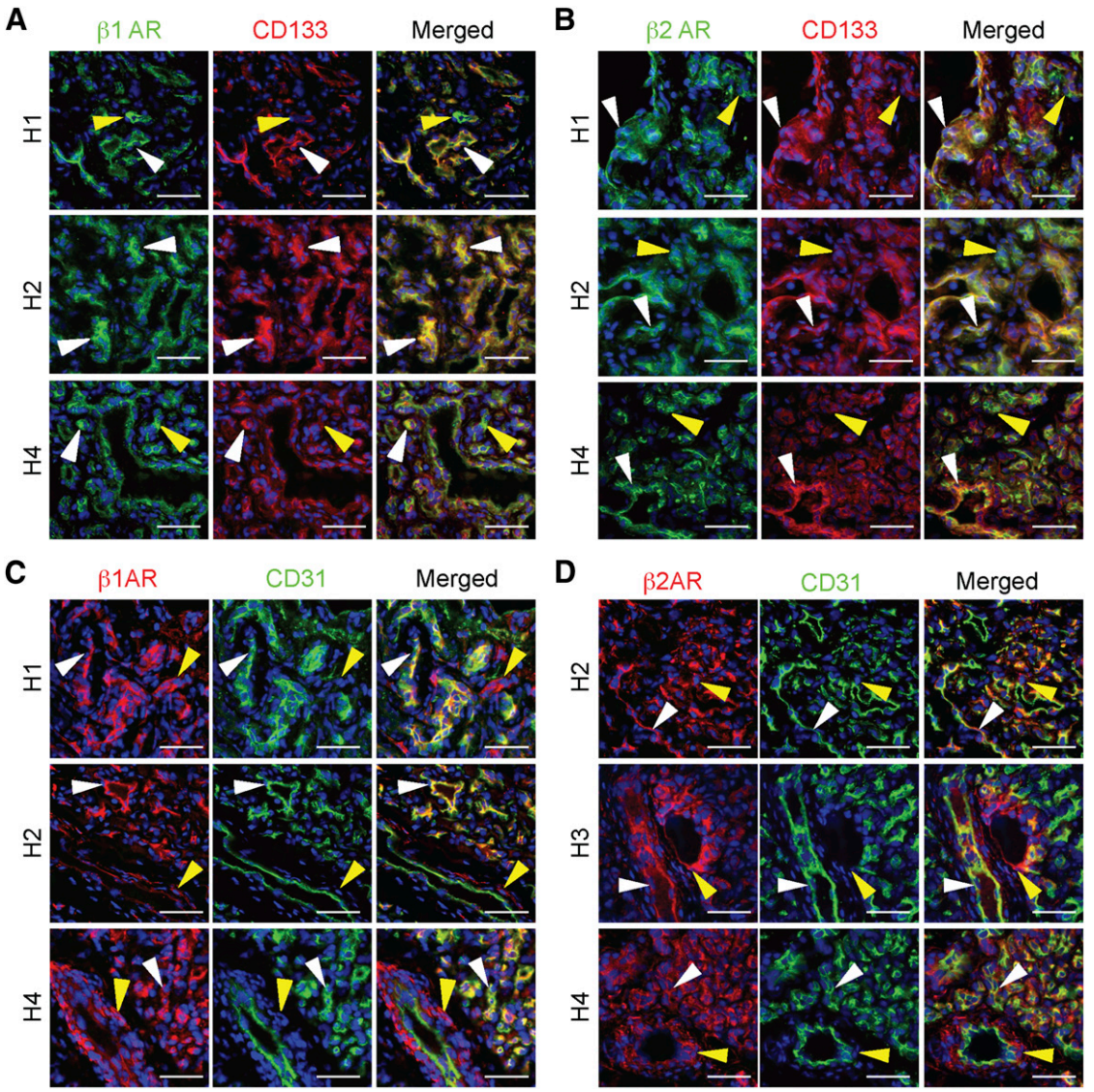


**Figure 1.** Hemangioma stem cells (HemSCs) and hemangioma endothelial cells (HemECs) in proliferating infantile hemangiomas (IHs) expressed $\beta$1AR and $\beta$2AR. IH tissue sections were costained for $\beta$1AR or $\beta$2AR and either a stem cell marker (CD133) or an endothelial cell marker (CD31) ($n$ = 7; representative images from three specimens shown). **(A):** $\beta$1AR and CD133 staining. White arrowheads mark $\beta$1AR-expressing CD133+ HemSCs. Yellow arrowheads mark cells that only express $\beta$1AR. **(B):** $\beta$2AR and CD133 staining. White arrowheads mark $\beta$2AR-expressing CD133+ HemSCs. Yellow arrowheads mark CD133− and $\beta$2AR+ cells. **(C):** $\beta$1AR and CD31 staining. White arrowheads mark $\beta$1AR-expressing CD31+ HemECs. Yellow arrowheads mark cells that only express $\beta$1AR localized to the perivascular region. **(D):** $\beta$2AR and CD31 staining. White arrowheads mark $\beta$2AR-expressing CD31+ HemECs. Yellow arrowheads mark CD31− and $\beta$2AR+ cells localized to perivascular regions. Scale bars = 50 $\mu$m. Abbreviations: $\beta$1AR, $\beta$1-adrenergic receptor; $\beta$2-adrenergic receptor.

the vehicle and propranolol treatment between the two cell populations. For all tests, $p < .05$ was considered statistically significant. Statistical analysis was performed using Minitab, version 16 (Minitab Inc., State College, PA, http://www.minitab.com).

## Results

### In IH Tissues HemSCs Expressed $\beta$1- and $\beta$2-Adrenergic Receptors

Because propranolol is a nonselective $\beta$AR antagonist with high affinity for the $\beta$1AR and $\beta$2AR [28], we determined their expression in HemSCs and HemECs in seven cutaneous proliferating hemangiomas. IH tissues are heterogeneous, and cells reside on a spectrum of CD133+ HemSCs localized adjacent to IH vessels and CD133+/CD31+ and CD31+ HemECs lining the IH vessels. $\beta$1AR was expressed in both CD133+ HemSCs and CD31+ HemECs (Fig. 1A, 1C). $\beta$2AR expression was strongest in CD133+ HemSCs, and only spotty expression was observed in HemECs (Fig. 1B, 1D). These results demonstrate that HemSCs in IHs express both $\beta$1AR and $\beta$2AR; thus, propranolol might be targeting the HemSCs, as well as the HemECs, in IH.

### Propranolol Dose Dependently Lowered cAMP Levels and Activated MAPK Signaling in HemSCs

Propranolol has been shown in non-IH cell types to both reduce cAMP levels and increase MAPK signaling downstream of $\beta$ARs

[24–28]. To investigate the downstream $\beta$AR signaling pathways affected by propranolol, HemSCs were treated with increasing amounts of propranolol and the cAMP levels and MAPK and ERK1/2 activity determined [17, 18, 36]. Increasing doses of the $\beta$AR agonist, isoprenaline, resulted in a significant increase in cAMP levels at 20 nM ($10^{-7.7}$ M) with an approximately threefold increase at 600 nM ($10^{-6.2}$ M; supplemental online Fig. 1A). To confirm that isoprenaline regulated cAMP levels via G$\alpha$s activation, we assessed the ability of isoprenaline to increase cAMP in the presence of 10 $\mu$M forskolin, a compound known to activate adenylyl cyclase. Isoprenaline was still able to increase cAMP levels in this assay, suggesting $\beta$AR signals via G$\alpha$s in HemSCs (supplemental online Fig. 1B). In contrast, increasing doses of propranolol steadily decreased the cAMP levels over a 7-log dose range, with significance observed at $10^{-10}$ M and maximum suppression reached at 100 nM ($10^{-7}$ M) propranolol (Fig. 2A).

Next, we determined the dose-dependent effects of propranolol on MAPK activity on HemSCs. HemSCs were treated with increasing amounts (7-log dose range) of propranolol, and ERK1/2 phosphorylation and total ERK expression were determined. Propranolol increased the total ERK1/2 levels in a dose-dependent manner (Fig. 2B). ERK1/2 activation was observed specifically at $10^{-5}$ M propranolol (Fig. 2B), consistent with a previous study in which propranolol activated ERK1/2 in 293T cells that ectopically expressed either $\beta$1AR or $\beta$2AR [28]. To assess whether the propranolol effects on ERK1/2 are specific to HemSCs, bone marrow-derived MSCs were treated with propranolol at 50 $\mu$M ($10^{-4.3}$ M) and 100 $\mu$M ($10^{-4}$ M). In MSCs, propranolol also increased ERK1/2 phosphorylation (supplemental online Fig. 2). Thus, high-dose propranolol increased ERK activation in multiple stem cell lines.

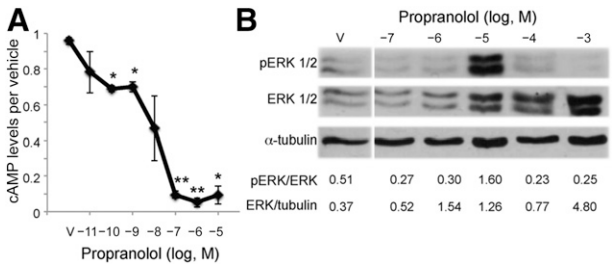


**Figure 2.** Propranolol dose dependently decreased cAMP levels and activated ERK1/2 in hemangioma stem cells (HemSCs). **(A):** HemSCs were treated with increasing doses of propranolol over a 7-log dose range ($10^{-11}$ M to $10^{-5}$ M) and cAMP levels determined. Data presented as the fold-difference between propranolol-treated HemSCs relative to vehicle-treated HemSCs $\pm$ SEM; *, $p < .005$; **, $p < .00002$. **(B):** HemSCs were treated with increasing doses of propranolol over a 5-log dose range ($10^{-7}$ M to $10^{-3}$ M), and ERK1/2 activation was determined at 30 minutes. Total and pERK1/2 expression was assessed by Western blot. Blots were serially stained for $\alpha$-tubulin as a protein-loading control. Ratios of total ERK1/2 to $\alpha$-tubulin and pERK1/2 to total ERK1/2 as determined by densitometry are presented below the blots. Abbreviations: ERK, extracellular signal-regulated kinase; pERK, phosphorylated ERK; V, vehicle.

## Propranolol Suppressed HemSC Proliferation and Induced HemSC Apoptosis and Cytotoxicity

We next investigated the effects of propranolol on HemSC proliferation and death. HemSCs were treated with either vehicle or increasing amounts of propranolol, ranging from $10^{-9}$ M to $10^{-3}$ M, and the total number of viable cells was determined after 24 and 48 hours. Vehicle-treated HemSCs grew 2.5-fold after 24 hours (Fig. 3A). A significant decrease of viable HemSCs was observed at $10^{-4}$ M propranolol after 24 hours and $10^{-9}$ M propranolol after 48 hours (Fig. 3A; supplemental online Fig. 3). At doses greater than $10^{-4}$ M propranolol, the number of viable cells decreased to less than the number of HemSCs at time 0 (supplemental online Fig. 3A), suggesting propranolol induced HemSC death, as well as suppressing their proliferation.

The effect of an 8-log dose range of propranolol on HemSC cytotoxicity was assessed using a DIMSCAN assay [35]. In this assay, drugs are introduced to confluent monolayers to assess cell survival independent of the drugs' effects on proliferation, and cytotoxicity is defined as less than 10% of HemSCs in the survival fraction [35]. After 24 hours, propranolol concentrations less than 100 $\mu$M ($10^{-4}$ M) did not significantly affect HemSC survival. At concentrations greater than 100 $\mu$M ($10^{-4}$ M), propranolol resulted in a sharp and significant decrease in the survival fraction (Fig. 3B). To more precisely determine the cytotoxic concentration of propranolol on HemSCs, a narrower range from 1 $\mu$M to 5 mM propranolol was assessed (Fig. 3C). After 24 hours, a significant reduction in HemSC survival was observed at 50 $\mu$M, and cytotoxicity was achieved at somewhere between 100 $\mu$M ($10^{-4}$ M) and 500 $\mu$M propranolol. HemSC survival was not observed (0% viability) at doses of $\geq$500 $\mu$M. The $LD_{50}$ of propranolol for HemSCs was determined to be approximately 200 $\mu$M, averaged from HemSCs isolated from 3 different IH specimens (supplemental online Table 1).

We used Annexin V and caspase-3 assays to determine whether propranolol-induced HemSC cell death occurred via an apoptotic pathway. Cell surface expression of Annexin V, a marker of active apoptosis, and propidium iodide incorporation, as a marker of dead cells, was determined by FACS analysis of HemSCs treated with vehicle or 50 $\mu$M, 100 $\mu$M, or 200 $\mu$M propranolol for 6 hours. Increasing doses of propranolol were associated with increased Annexin V positivity (Fig. 3D). An increase in HemSC apoptosis was not observed when cells were exposed to propranolol for more than 48 hours, suggesting propranolol rapidly induced HemSC apoptosis (data not shown). To confirm the Annexin V results, caspase-3 activity, a marker of apoptosis, was determined in HemSCs treated with vehicle or 50 $\mu$M, 200 $\mu$M, or 400 $\mu$M propranolol (cytotoxicity at $LD_{10}$, $LD_{50}$, and $LD_{90}$, respectively) in the presence or absence of serum for 24 hours. A significant increase in caspase-3 activity was observed at 100 $\mu$M propranolol that increased with the higher propranolol concentrations (supplemental online Fig. 4). Thus, cytotoxic doses of propranolol ($>10^{-4}$ M) significantly increased Annexin V positivity and caspase-3 activation, suggesting propranolol rapidly induces HemSC apoptosis.

## Propranolol's Antiproliferative Effects in HemSCs Are Mediated via $\beta$ARs

We previously showed that isolated HemSCs express $\beta$1AR and $\beta$2AR and that propranolol inhibited HemSC proliferation [21]. We screened $\beta$1AR and $\beta$2AR transcript levels in the HemSC populations ($n$ = 8) and found that most HemSC populations expressed high levels of $\beta$2AR and low levels of $\beta$1AR, including those used for the present studies (supplemental online Table 1).

To investigate whether the propranolol effects on HemSCs are mediated via perturbation of $\beta$AR signaling, HemSCs were

 

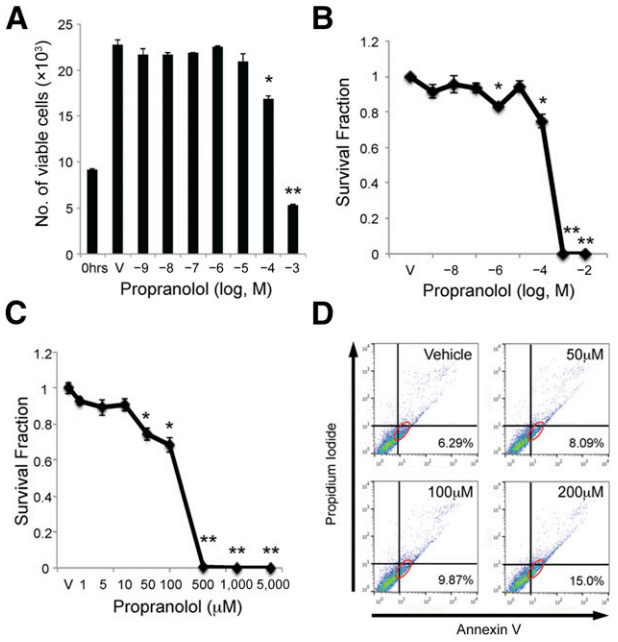


**Figure 3.** Propranolol inhibited proliferation and induced apoptosis of hemangioma stem cells (HemSCs). **(A):** HemSCs were treated with increasing doses of propranolol over a 10-log dose range and the number of viable HemSCs determined at time 0 before treatment or 24 hours after treatment. *, $p < .002$ and **, $p < .001$ compared with vehicle. **(B):** HemSCs were treated with increasing doses of propranolol over an 8-log dose range ($10^{-9}$ M to $10^{-2}$ M), and viability was assessed by Digital Imaging Microscopy System (DIMSCAN) assay at 24 hours. *, $p < .0005$; **, $p < .000001$. **(C):** HemSCs were treated with increasing doses of propranolol from 1 $\mu$M to 5 mM, and viability was assessed by DIMSCAN assay at 24 hours. *, $p < .001$; **, $p < .00001$. **(B, C):** Data presented as survival fraction of propranolol-treated HemSCs relative to vehicle controls ± SEM. **(D):** HemSCs were treated with 50 $\mu$M, 200 $\mu$M, and 400 $\mu$M propranolol (corresponding to $LD_{10}$, $LD_{50}$, and $LD_{90}$), and Annexin V assay was performed at 24 hours. Annexin V detects actively apoptotic cells (*x*-axis), and propidium iodide (*y*-axis) detects necrotic cells. Annexin V-positive and propidium iodide-negative apoptotic HemSCs are circled in red and their percentages shown in the lower right corner. Abbreviation: V, vehicle.

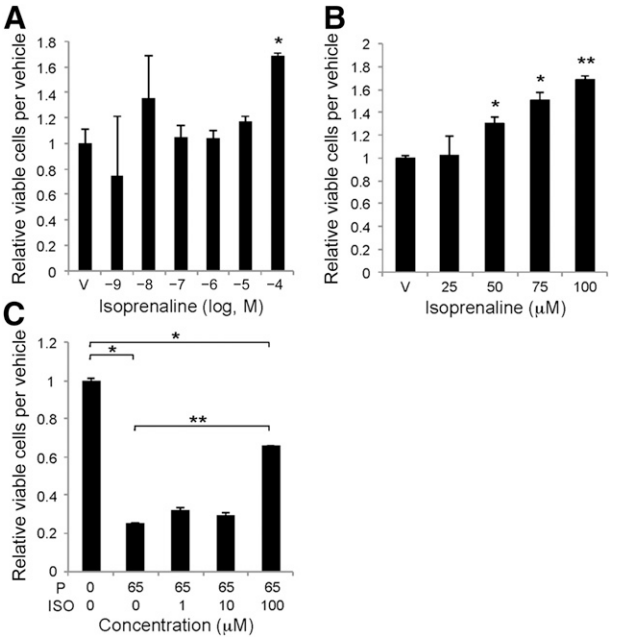


**Figure 4.** Isoprenaline induced hemangioma stem cell (HemSC) proliferation and blocked propranolol's antiproliferative effects on HemSCs. **(A):** HemSCs were treated with increasing doses of isoprenaline over a 6-log dose range ($10^{-9}$ M to $10^{-4}$ M), and proliferation was determined at 48 hours. *, $p < .05$. **(B):** HemSCs were treated with a narrower dose range of isoprenaline from 25 $\mu$M to 100 $\mu$M ($10^{-4.6}$ M to $10^{-4}$ M), and proliferation was determined at 48 hours. *, $p < .05$; **, $p < .005$. **(C):** HemSCs were pretreated with increasing doses of isoprenaline for 1 hour. Next, 65 $\mu$M propranolol (antiproliferative dose) was added and proliferation determined at 24 hours. *, $p < .05$; **, $p < .0005$. **(A–C):** Data presented as fold-difference to vehicle-treated HemSCs ± SEM. Abbreviations: ISO, isoprenaline; P, propranolol; V, vehicle.

treated with increasing amounts of the $\beta$AR-specific agonist, isoprenaline, over a 6-log dose range, and proliferation was determined at 48 hours. A dose of $10^{-4}$ M isoprenaline resulted in an ~1.7-fold increase in HemSC proliferation (Fig. 4A). In a narrower dose range from 25 to 100 $\mu$M, significant HemSC proliferation was induced at 50 $\mu$M ($10^{-4.3}$ M) isoprenaline (Fig. 4B). We determined the ability of increasing amounts of isoprenaline to reverse the antiproliferative effects of propranolol after 24 hours. A dose of 100 $\mu$M ($10^{-4}$ M) isoprenaline significantly increased HemSC proliferation—2.64-fold in the presence of 65 $\mu$M ($10^{-4.2}$ M) propranolol relative to 65 $\mu$M propranolol alone (Fig. 4C). However, HemSC proliferation was still significantly decreased relative to the vehicle-treated cells, suggesting that the propranolol effects on HemSC proliferation were mediated by both $\beta$AR-dependent and $\beta$AR-independent mechanisms.

## A cAMP Analog or MAPK Inhibition Partially Rescued Propranolol Effects on HemSCs

At $10^{-5}$ M propranolol, suppression of cAMP levels and ERK activation (Fig. 2) correlated with the antiproliferative and antisurvival effects of propranolol (Fig. 3). To determine whether these two signaling events were necessary for propranolol to exert its cellular effects, HemSC proliferation and survival was assessed in the presence of bucladesine, a cAMP analog, or U0126, a MEK1/2 inhibitor. U0126 partially rescued the decrease in cell viability caused by100 $\mu$M propranolol, but bucladesine did not (Fig. 5A; data not shown). To determine whether cAMP suppression was necessary for propranolol-induced cytotoxicity at doses greater than $10^{-4}$ M, increasing doses of bucladesine were added to HemSCs exposed to 200 $\mu$M propranolol ($LD_{50}$), and HemSC survival was assessed at 24 hours. At 100 $\mu$M, bucladesine partially reversed propranolol-induced HemSC cytotoxicity, suggesting that cAMP suppression was necessary for HemSC death at higher concentrations ($\geq 10^{-4}$ M; Fig. 5B). U0126 alone did not affect HemSC survival, but it did partially rescue propranolol-induced cell death (Fig. 5C). Together, these results demonstrate that propranolol via MAPK activation inhibited HemSC proliferation, and both cAMP suppression and MAPK activation mediated propranolol-induced HemSC cell death.

## Propranolol Effects on HemSCs Were Mediated via Inhibition of $\beta$2AR

The HemSC populations studied expressed high levels $\beta$2AR and low levels of $\beta$1AR (supplemental online Table 1). We

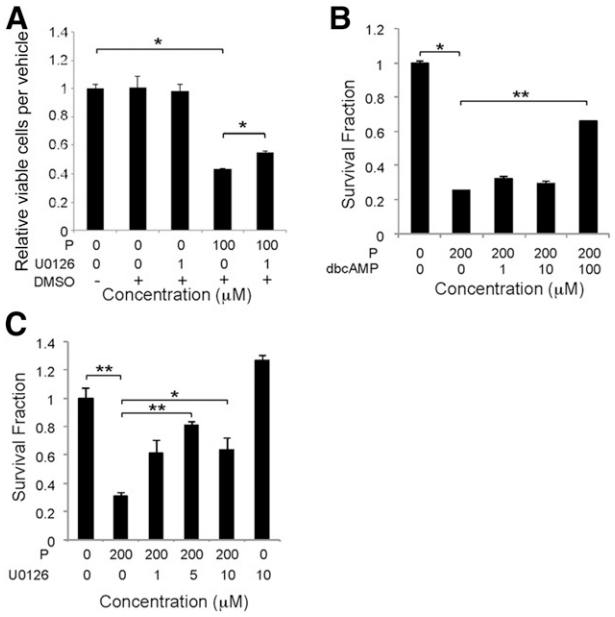


**Figure 5.** Ectopic cAMP or mitogen-activated protein kinase inhibition partially rescued the propranolol-induced effects on hemangioma stem cells (HemSCs). **(A):** HemSCs, in either the presence or absence of 100 $\mu$M propranolol were treated with 1 $\mu$M U0126 or DMSO as a vehicle control, and the number of viable HemSCs was determined at 48 hours. $*$, $p < .05$. Data presented as fold-difference between treatment group and control $\pm$ SEM. **(B):** HemSCs, in either the presence or absence of 200 $\mu$M propranolol (proapoptotic dose), were treated with increasing doses of dbcAMP, and cell viability was determined by Digital Imaging Microscopy System (DIMSCAN) at 24 hours. $*$, $p < .02$; $**$, $p < .0001$. **(C):** HemSCs, either in the presence or absence of 200 $\mu$M propranolol (proapoptotic dose), were treated with increasing doses of U0126, and cell viability was determined by DIMSCAN at 24 hours. $*$, $p < .05$; $**$, $p < .005$. Data presented as survival fraction relative to control $\pm$ SEM **(B, C)**. Abbreviations: dbcAMP, dibutyryl cAMP; DMSO, dimethyl sulfoxide; P, propranolol.

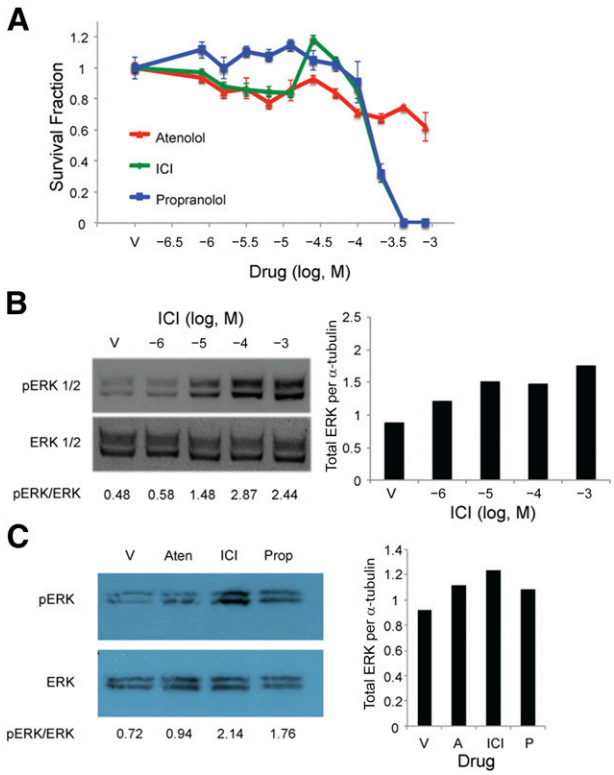


**Figure 6.** $\beta$2-Adrenergic receptor inhibition mirrored propranolol's effects on hemangioma stem cell (HemSC) viability and ERK1/2 activation. **(A):** HemSCs were treated with increasing doses of atenolol, ICI, or propranolol ($10^{-6.5}$ M to $10^{-3}$ M), and HemSC viability was assessed by Digital Imaging Microscopy System (DIMSCAN) assay at 24 hours. Data presented as survival fraction of propranolol-treated HemSCs relative to vehicle controls $\pm$ SEM. At doses of 200 $\mu$M propranolol or greater, HemSC viability was significantly greater for cells treated with atenolol compared with those treated with either ICI or propranolol ($p < .005$ at 200 $\mu$M, $p < .001$ at 400 $\mu$M, and $p < .005$ at 800 $\mu$M). No significant difference was seen in cell viability between the cells treated with ICI and propranolol. **(B):** HemSCs were treated with increasing doses of ICI over a 4-log dose range ($10^{-6}$ M to $10^{-3}$ M), and ERK1/2 activation was determined at 30 minutes by Western blot. **(C):** HemSCs were treated with 100 $\mu$M atenolol, ICI, or propranolol, and ERK1/2 activation was determined at 30 minutes by Western blot. **(B, C):** Blots were serially stained for $\alpha$-tubulin as a protein-loading control. Ratios of pERK1/2 to total ERK1/2 as determined by densitometry are presented below the blots. Ratio of total ERK1/2 to $\alpha$-tubulin presented in bar graphs to the right. Abbreviations: A, atenolol; Aten, atenolol; ERK, extracellular signal-regulated kinase; pERK, phosphorylated ERK; ICI, ICI-118,551; P, propranolol; Prop, propranolol; V, vehicle.

investigated whether the $\beta$2AR-specific antagonist, ICI-118,551 had similar effects on HemSCs, because propranolol is a pan-$\beta$AR antagonist, and compared its effects with that of the $\beta$1AR-specific antagonist, atenolol. HemSCs were exposed to a 4-log dose of propranolol (pan-$\beta$AR antagonist), atenolol ($\beta$1AR-specific antagonist), and ICI 118,551 ($\beta$2AR-specific antagonist). HemSC survival was determined after 24 hours. ICI mirrored the propranolol cytotoxic effects on HemSCs at $10^{-4}$ M to $10^{-3}$ M (Fig. 6A). Although atenolol modestly decreased cell viability (Fig. 6A), the effects of atenolol were similar to those observed for vehicle (DMSO) alone, indicating that the reduced HemSC survival resulted from DMSO and not the $\beta$1AR-specific antagonist (supplemental online Fig. 5). The effects of either propranolol or ICI when compared individually with atenolol on HemSC survival were statistically significant by ANOVA at 200 $\mu$M, 400 $\mu$M, and 800 $\mu$M ($10^{-3.09}$ M, $10^{-3.39}$ M, $10^{-3.69}$ M, respectively). In contrast, no significant difference was seen in the fold-change in the cytotoxic effects between ICI and propranolol, suggesting propranolol targets $\beta$2AR in HemSCs. We observed a similar response in MSCs, in which ICI induced significant MSC cytotoxicity, similar to that of propranolol, which was not observed with atenolol (supplemental online Fig. 6A). MSCs also expressed higher levels of $\beta$2AR transcripts compared with $\beta$1AR (data not shown).

The effect of ICI on HemSC proliferation relative to propranolol and atenolol was tested. After 72 hours, 100 $\mu$M ICI reduced the number of viable HemSCs similar to that observed for propranolol (supplemental online Fig. 6B). The $\beta$1AR-specific antagonists, atenolol and metoprolol, did not affect HemSC cell viability in this assay (supplemental online Fig. 6B; data not shown).

We next assessed the effects of $\beta$1AR versus $\beta$2AR inhibition on ERK1/2 activation. ICI treatment of HemSCs increased total ERK expression and activated ERK1/2 at $10^{-5}$ M through $10^{-3}$ M (Fig. 6B, 6C). Although a slight increase in total ERK was observed, 100 $\mu$M atenolol did not activate ERK1/2 in HemSCs (Fig. 6C). Taken together, $\beta$2AR-specific antagonism

 

of HemSCs mirrored the antiproliferative, antisurvival, and ERK1/2 activation effects of propranolol, suggesting propranolol targets $\beta$2AR in HemSCs to elicit its biological effects.

### Propranolol Affects Vascular Development in a Xenograft Mouse Model of IH

To assess how propranolol affects HemSCs and IH development in vivo, we adapted a previously described mouse model [20]. In the IH mouse model, HemSCs resuspended in Matrigel are implanted subcutaneously in immunocompromised mice, and IH vessel development progresses over 3 weeks. The mice were treated with propranolol or vehicle 40 mg/kg daily. Using the surface area conversion factor of 1/12 [37–39], the mice received a human equivalent dose of 3.3–4.8 mg/kg daily. IH Matrigel implants from propranolol-treated mice had reduced blood flow at 14 and 21 days after implantation, measured by Doppler ultrasound, compared with vehicle (data not shown; Fig. 7A). Histological analysis of the 21-day IH Matrigel implants (Fig. 7B) demonstrated that propranolol did not affect blood vessel density (Fig. 7C) but did significantly reduce the vessel diameter relative to the vehicle-treated implants (Fig. 7D). The reduced vessel caliber correlated with a loss of Doppler-detectable flow in the propranolol treatment group. Propranolol also significantly increased the number of cells that expressed phosphorylated ERK1/2 within the IH Matrigel implant (Fig. 7E), consistent with the results from our in vitro studies. Thus, propranolol improved vessel development in the IH mouse model that correlated with MAPK pathway activation.

## Discussion

In IH tissues, HemSCs expressed both $\beta$1AR and $\beta$2AR. In isolated HemSCs, propranolol treatment dose dependently decreased cAMP levels and activated the MAPK pathway downstream of $\beta$ARs. At low doses ($IC_{50}$ of 65 $\mu$M), propranolol decreased cell viability by inhibiting HemSC proliferation and promoting HemSC apoptosis. In contrast, at high doses ($LD_{50}$ of 200 $\mu$M [$10^{-3.7}$ M]), propranolol was cytotoxic against HemSCs. The $\beta$AR agonist, isoprenaline, a cAMP analog, and a MAPK inhibitor partially rescued the propranolol-induced antiproliferative and antisurvival effects on HemSCs. The $\beta$2AR-specific antagonist, ICI-118,551, mirrored the propranolol effects on HemSC proliferation and survival of HemSCs. In an IH mouse model, propranolol reduced abnormal vessel dilation and increased p-ERK expression. Taken together, these data demonstrated that the propranolol effects on HemSCs are mediated in part via $\beta$2AR inhibition and suggest a role for $\beta$2AR signaling and its downstream cAMP and MAPK pathways in HemSC pathophysiology.

Both activation and inactivation of $\beta$AR has been shown to induce MAPK signaling. This could occur because multiple pathways downstream of $\beta$AR lead to activation of the downstream MAPK pathway. MAPK activation downstream of $\beta$AR stimulation can occur downstream of a G$\alpha$S/AC/cAMP/PKA pathway [28] or through a G$\beta/\gamma$/Ras pathway [24–27]. Alternatively, propranolol, a $\beta$AR antagonist, has been shown to also lead to MAPK activation, possibly by disrupting $\beta$-arrestin function in decreasing the MAPK activity induced by G-protein-dependent pathways [29, 30, 32, 33, 40]. We found that propranolol activated ERK1/2 in isolated HemSCs and in an IH mouse model. The addition of an MEK inhibitor blocked the propranolol antiproliferative and antisurvival effects on HemSCs, suggesting that propranolol uses MAPK signal activation downstream of $\beta$AR inhibition to mediate its effects on HemSCs. Moreover, ICI mirrored the propranolol effects on ERK1/2 activation, suggesting that propranolol activates the MAPK pathway via inhibition of $\beta$2AR in HemSCs. This is consistent with the findings from previous studies, which have shown that propranolol activates MAPK through $\beta$2ARs [30, 33].

We found that high-dose propranolol rapidly induced HemSC apoptosis, with induction observed within 6 hours by Annexin V assay and 24 hours by caspase-3 assay. This is in contrast to previous studies, in which it was shown that propranolol induced HemSC death by a nonapoptotic pathway [21, 23, 41]. The difference between the present study and others mostly likely resulted from the timing of the apoptosis assessment. Kum and Khan [23] assessed the propranolol effects on apoptosis after 72 hours of propranolol treatment. In contrast, we reported that surface Annexin V expression was not increased at 24 hours of treatment [21, 41]. Annexin V can only be detected in cells actively undergoing apoptosis; thus, we believe we did not assess apoptosis at the appropriate time, because most cells were already dead, confirmed by propidium iodide incorporation. The results we have presented have demonstrated that $>50$ $\mu$M propranolol rapidly induced HemSC apoptosis within 6–24 hours of treatment. Propranolol cytotoxicity was observed at propranolol concentrations of $10^{-4}$ M.

The clinically used dosage of propranolol for IH treatment ranges from 1 to 3 mg/kg daily [11, 42, 43]. Although the serum concentration of propranolol in IH-treated infants has not been published, the plasma concentrations for adults taking 0.5–1.5 mg/kg per day ranged from $10^{-6.8}$ M to $10^{-6.3}$ M [44, 45]. In the present study, the clinical relative dose range of $10^{-6.5}$ M to $10^{-5.8}$ M propranolol both inhibited HemSC proliferation and induced HemSC apoptosis. However, this dose range is less than the concentration necessary to induce HemSC cytotoxicity. Thus, it is possible that the current propranolol dosing in IH patients reduces HemSC numbers but might allow for residual pools of IH stem cells, which might contribute to regrowth. IH rebound has been observed in as high as 25% of patients after discontinuation of propranolol therapy [46]. Thus, increasing the dose of propranolol given to patients with IH might induce HemSC cytotoxicity and prevent the rebound observed with propranolol discontinuation. In support of this idea, we found improved vessel morphology in the IH mouse model at a human equivalent dose of propranolol of 3.3–4.8 mg/kg per day.

Different cell populations in IHs express different levels of $\beta$AR subtypes, with high levels of $\beta$2AR expression seen in HemSCs and IH-derived pericytes [19]. In contrast, $\beta$1AR and $\beta$2AR are equally expressed in HemECs [17]. We have demonstrated that HemSCs in tissues express both $\beta$1AR and $\beta$2AR, but cultured HemSCs predominantly express $\beta$2AR. Propranolol has been suggested to target HemECs [17, 21, 47, 48] and hemangioma-derived pericytes [19], and the present study and others [21–23, 41] have demonstrated that propranolol also targets HemSCs. Thus, propranolol mediates its effects by targeting multiple cell types in IHs.

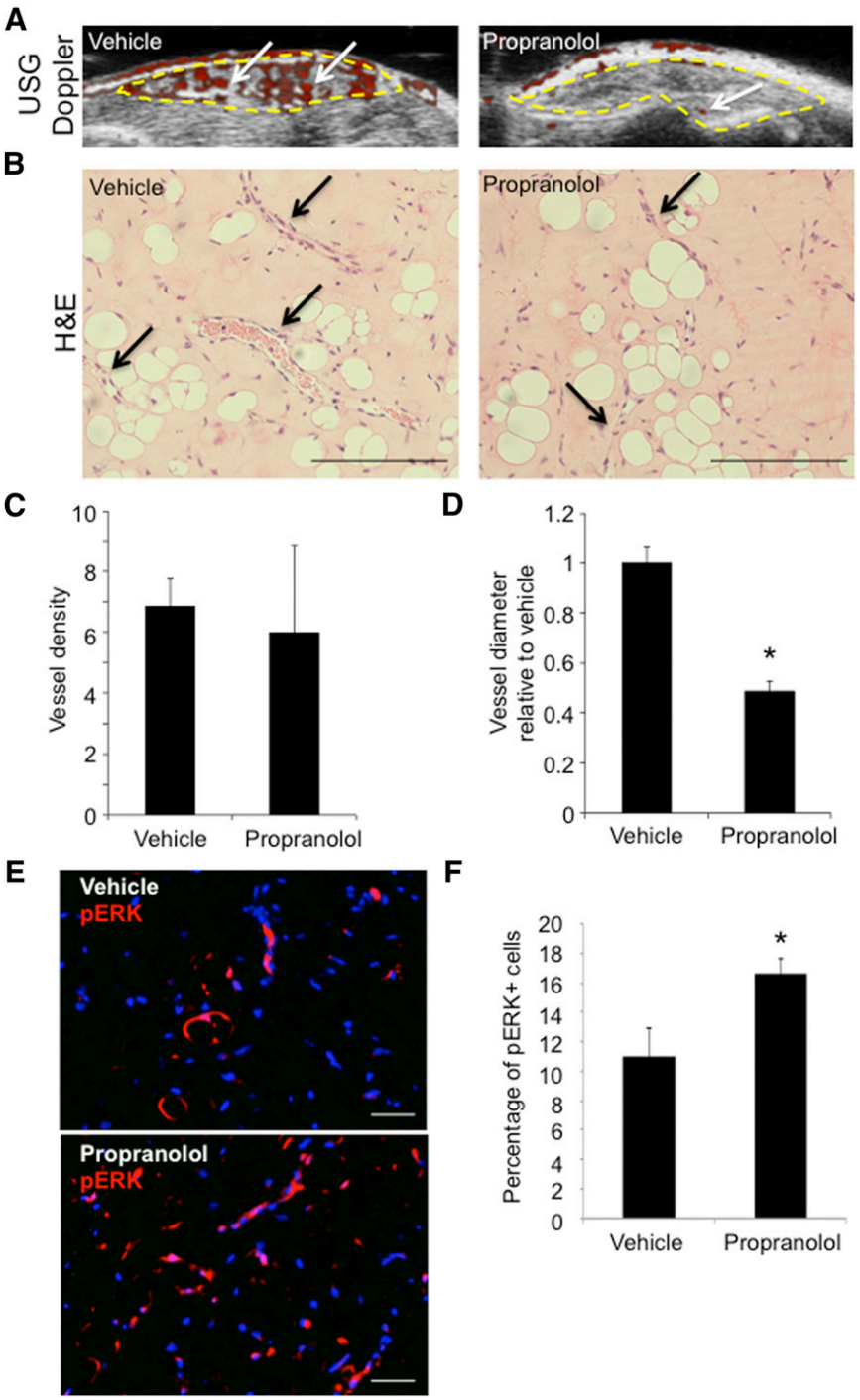


**Figure 7.** Propranolol reduced vessel caliber and increased ERK1/2 phosphorylation in an infantile hemangioma (IH) mouse model. Hemangioma stem cell (HemSC) Matrigel implants were xenografted into the flanks of immunocompromised mice, which were split into two treatment groups: vehicle and propranolol for 3 weeks ($n = 2$ cell populations; four Matrigel implants per treatment group). **(A):** Ultrasound-guided Doppler of implants at 21 days after implantation demonstrated reduced blood flow (red; white arrows) in implants from the propranolol treatment group compared with vehicle. **(B):** H&E of implant sections at 21 days after implantation. Black arrows highlight blood vessels. **(C):** Quantification of average blood vessel number per high-power field (HPF) in implants from vehicle and propranolol treatment. **(D):** Quantification of average blood vessel diameter in propranolol-treated group compared with vehicle for both H49 and H50. $*$, $p < .0001$ **(C, D)**; $n = 4$–5 HPF for each line and treatment. **(E):** Vehicle- and propranolol-treated implants stained for pERK1/2. **(F):** Quantification of the number of pERK1/2-positive cells divided by the total number of cells. $*$, $p < .05$. Scale bars = 50 $\mu$m. Abbreviations: ERK, extracellular signal-regulated kinase; pERK, phosphorylated ERK; USG, ultrasonography.

Our in vitro data have demonstrated that a $\beta$2AR-specific, but not $\beta$1AR-specific, antagonist replicated the propranolol effects in HemSCs, suggesting that inhibition of $\beta$2AR activity alone is sufficient for the propranolol effects against HemSCs. Alternatively, the low $\beta$1AR expression in cultured HemSCs might be responsible for the absence of $\beta$1AR-specific antagonist responses.

 

Further studies using $\beta$AR-specific antagonists in the IH mouse model might address this issue more effectively. Anecdotal clinical reports of using $\beta$1AR-specific antagonists in 3 cases of subglottic hemangiomas had mixed success [49]. However, a $\beta$1AR-specific antagonist might not effectively target HemSCs and IH-derived pericytes that also express $\beta$2AR.

## Conclusion

Our study has provided important details for understanding the mechanism of propranolol action in the treatment of IH. Although propranolol affects HemSCs in part by disrupting $\beta$AR signaling, likely $\beta$2AR, a number of questions regarding the antiproliferative and cytotoxic effects of propranolol remain unanswered, including whether propranolol targets other receptor pathways to affect proliferation or cell viability. Given our findings, the possibility of targets other than $\beta$ARs remains a possibility, especially at the high, cytotoxic dose. We are in the process of investigating these possibilities, and our findings could further enhance our understanding of the mechanism of action of propranolol in IH treatment and allow for the development of more effective treatment strategies.

## Acknowledgments

This work was supported by NIH Grant K08 1K08 HL102068-01 and Columbia University CTSA Grant UL1 TR000040 to J.K.W., NIH Grant 1R21 EB016515-01 to C.J.S., NIH Grant 1R01 HL112626 to J.K.K., and NIH Grant T35 5T35HL007616-34 to R.W.E. We thank Valeriya Borishenko for technical assistance.

## Author Contributions

N.C.O.M. and R.W.E.: performance of experiments, generation and assembly of data, manuscript writing; A.K.E. and A.A.K.: performance of experiments, generation and assembly of data; Q.K.T., J.E.K., and M.W.: performance of experiments, generation of data; A.W.: statistical analysis; J.K.K.: financial support, data analysis and interpretation, final approval of manuscript; C.J.S. and J.K.W.: conception and design, financial support, manuscript writing, data analysis and interpretation, final approval of manuscript.

## Disclosure of Potential Conflicts of Interest

The authors indicated no potential conflicts of interest.

## References

1 Mulliken JB, Fishman SJ, Burrows PE. Vascular anomalies. Curr Probl Surg 2000;37:517–584.

2 Frieden IJ, Haggstrom AN, Drolet BA et al. Infantile hemangiomas: Current knowledge, future directions. Proceedings of a research workshop on infantile hemangiomas, April 7–9, 2005, Bethesda, Maryland, USA. Pediatr Dermatol 2005;22:383–406.

3 Kwon EK, Seefeldt M, Drolet BA. Infantile hemangiomas: An update. Am J Clin Dermatol 2013;14:111–123.

4 Chamlin SL, Haggstrom AN, Drolet BA et al. Multicenter prospective study of ulcerated hemangiomas. J Pediatr 2007;151:684–689.

5 Haggstrom AN, Drolet BA, Baselga E et al. Prospective study of infantile hemangiomas: Clinical characteristics predicting complications and treatment. Pediatrics 2006;118:882–887.

6 Boon LM, Burrows PE, Paltiel HJ et al. Hepatic vascular anomalies in infancy: A twenty-seven-year experience. J Pediatr 1996;129:346–354.

7 Arneja JS, Mulliken JB. Resection of amblyogenic periocular hemangiomas: Indications and outcomes. Plast Reconstr Surg 2010;125:274–281.

8 Bitar MA, Moukarbel RV, Zalzal GH. Management of congenital subglottic hemangioma: Trends and success over the past 17 years. Otolaryngol Head Neck Surg 2005;132:226–231.

9 Léauté-Labrèze C, Dumas de la Roque E, Hubiche T et al. Propranolol for severe hemangiomas of infancy. N Engl J Med 2008;358:2649–2651.

10 Sans V, de la Roque ED, Berge J et al. Propranolol for severe infantile hemangiomas: Follow-up report. Pediatrics 2009;124:e423–e431.

11 Lou Y, Peng WJ, Cao Y et al. The effectiveness of propranolol in treating infantile haemangiomas: A meta-analysis including 35 studies. Br J Clin Pharmacol 2014;78:44–57.

12 Hogeling M, Adams S, Wargon O. A randomized controlled trial of propranolol for infantile hemangiomas. Pediatrics 2011;128:e259–e266.

13 Bauman NM, McCarter RJ, Guzzetta PC et al. Propranolol vs prednisolone for symptomatic proliferating infantile hemangiomas: A randomized clinical trial. JAMA Otolaryngol Head Neck Surg 2014;140:323–330.

14 Frieden IJ, Drolet BA. Propranolol for infantile hemangiomas: Promise, peril, pathogenesis. Pediatr Dermatol 2009;26:642–644.

15 Lawley LP, Siegfried E, Todd JL. Propranolol treatment for hemangioma of infancy: Risks and recommendations. Pediatr Dermatol 2009;26:610–614.

16 Storch CH, Hoeger PH. Propranolol for infantile haemangiomas: Insights into the molecular mechanisms of action. Br J Dermatol 2010;163:269–274.

17 Chim H, Armijo BS, Miller E et al. Propranolol induces regression of hemangioma cells through HIF-1$\alpha$-mediated inhibition of VEGF-A. Ann Surg 2012;256:146–156.

18 Ji Y, Chen S, Li K et al. The role of $\beta$-adrenergic receptor signaling in the proliferation of hemangioma-derived endothelial cells. Cell Div 2013;8:1.

19 Lee D, Boscolo E, Durham JT et al. Propranolol targets the contractility of infantile haemangioma-derived pericytes. Br J Dermatol 2014;171:1129–1137.

20 Khan ZA, Boscolo E, Picard A et al. Multipotential stem cells recapitulate human infantile hemangioma in immunodeficient mice. J Clin Invest 2008;118:2592–2599.

21 Wong A, Hardy KL, Kitajewski AM et al. Propranolol accelerates adipogenesis in hemangioma stem cells and causes apoptosis of hemangioma endothelial cells. Plast Reconstr Surg 2012;130:1012–1021.

22 Zhang L, Mai HM, Zheng J et al. Propranolol inhibits angiogenesis via down-regulating the expression of vascular endothelial growth factor in hemangioma derived stem cell. Int J Clin Exp Pathol 2014;7:48–55.

23 Kum JJ, Khan ZA. Propranolol inhibits growth of hemangioma-initiating cells but does not induce apoptosis. Pediatr Res 2014;75:381–388.

24 Hentrich F, Göthert M, Greschuchna D. Involvement of cAMP in modulation of noradrenaline release in the human pulmonary artery. Naunyn Schmiedebergs Arch Pharmacol 1985;330:245–247.

25 Bockaert J, Pin JP. Molecular tinkering of G protein-coupled receptors: An evolutionary success. EMBO J 1999;18:1723–1729.

26 Bruni P, Burns DL, Hewlett EL et al. Effects of pertussis toxin on cAMP and cGMP responses to carbamylcholine in N1E-115 neuroblastoma cells. Mol Pharmacol 1985;28:229–234.

27 Li H, Fong C, Chen Y et al. Beta-adrenergic signals regulate adipogenesis of mouse mesenchymal stem cells via cAMP/PKA pathway. Mol Cell Endocrinol 2010;323:201–207.

28 Galandrin S, Bouvier M. Distinct signaling profiles of beta1 and beta2 adrenergic receptor ligands toward adenylyl cyclase and mitogen-activated protein kinase reveals the pluridimensionality of efficacy. Mol Pharmacol 2006;70:1575–1584.

29 Azzi M, Charest PG, Angers S et al. Beta-arrestin-mediated activation of MAPK by inverse agonists reveals distinct active conformations for G protein-coupled receptors. Proc Natl Acad Sci USA 2003;100:11406–11411.

30 Baker JG, Hall IP, Hill SJ. Agonist and inverse agonist actions of beta-blockers at the human beta 2-adrenoceptor provide evidence for agonist-directed signaling. Mol Pharmacol 2003;64:1357–1369.

31 Kenakin T. Principles: Receptor theory in pharmacology. Trends Pharmacol Sci 2004;25:186–192.

**32** Wisler JW, DeWire SM, Whalen EJ et al. A unique mechanism of beta-blocker action: Carvedilol stimulates beta-arrestin signaling. Proc Natl Acad Sci USA 2007;104:16657–16662.

**33** Nobles KN, Xiao K, Ahn S et al. Distinct phosphorylation sites on the $\beta$(2)-adrenergic receptor establish a barcode that encodes differential functions of $\beta$-arrestin. Sci Signal 2011;4:ra51.

**34** Wu JK, Adepoju O, De Silva D et al. A switch in Notch gene expression parallels stem cell to endothelial transition in infantile hemangioma. Angiogenesis 2010;13:15–23.

**35** Keshelava N, Frgala T, Krejsa J et al. DIMSCAN: A microcomputer fluorescence-based cytotoxicity assay for preclinical testing of combination chemotherapy. Methods Mol Med 2005;110:139–153.

**36** Lamy S, Lachambre MP, Lord-Dufour S et al. Propranolol suppresses angiogenesis in vitro: Inhibition of proliferation, migration, and differentiation of endothelial cells. Vascul Pharmacol 2010;53:200–208.

**37** Freireich EJ, Gehan EA, Rall DP et al. Quantitative comparison of toxicity of anticancer agents in mouse, rat, hamster, dog, monkey, and man. Cancer Chemother Rep 1966;50: 219–244.

**38** Reagan-Shaw S, Nihal M, Ahmad N. Dose translation from animal to human studies revisited. FASEB J 2008;22:659–661.

**39** U.S. National Institutes of Health. Equivalent Surface Area Dosage Conversion Factors. Available at https://ncifrederick.cancer.gov/lasp/acuc/frederick/Media/Documents/ACUC42.pdf. Accessed April 16, 2015.

**40** Luttrell LM, Lefkowitz RJ. The role of beta-arrestins in the termination and transduction of G-protein-coupled receptor signals. J Cell Sci 2002;115:455–465.

**41** England RW, Hardy KL, Kitajewski AM et al. Propranolol promotes accelerated and dysregulated adipogenesis in hemangioma stem cells. Ann Plast Surg 2014;73(suppl 1): S119–S124.

**42** Drolet BA, Frommelt PC, Chamlin SL et al. Initiation and use of propranolol for infantile hemangioma: Report of a consensus conference. Pediatrics 2013;131:128–140.

**43** Léauté-Labrèze C, Hoeger P, Mazereeuw-Hautier J et al. A randomized, controlled trial of oral propranolol in infantile hemangioma. N Engl J Med 2015;372:735–746.

**44** Wong L, Nation RL, Chiou WL et al. Plasma concentrations of propranolol and 4-hydroxypropranolol during chronic oral propranolol therapy. Br J Clin Pharmacol 1979; 8:163–167.

**45** Mansur AP, Avakian SD, Paula RS et al. Pharmacokinetics and pharmacodynamics of propranolol in hypertensive patients after sublingual administration: Systemic availability. Braz J Med Biol Res 1998;31: 691–696.

**46** Shah S, Frieden I, Baselga E et al. Rebound after discountinuation of propranolol in the therapy of infantile hemangiomas: A retrospective study. Paper presented at: 20th International Workshop on Vascular Anomalies; April 1–4, 2014; Melbourne, Victoria, Australia.

**47** Stiles J, Amaya C, Pham R et al. Propranolol treatment of infantile hemangioma endothelial cells: A molecular analysis. Exp Ther Med 2012;4:594–604.

**48** Ji Y, Li K, Xiao X et al. Effects of propranolol on the proliferation and apoptosis of hemangioma-derived endothelial cells. J Pediatr Surg 2012;47:2216–2223.

**49** Blanchet C, Nicollas R, Bigorre M et al. Management of infantile subglottic hemangioma: Acebutolol or propranolol? Int J Pediatr Otorhinolaryngol 2010;74: 959–961.

See www.StemCellsTM.com for supporting information available online.

 